

Authors' response to Referee 3

Journal: Ocean Sciences

Title of paper: Impact of intraseasonal wind bursts on SST variability in the far eastern Tropical Atlantic Ocean during boreal spring 2005 and 2006. Focus on the mid-May 2005 event.

Authors: Herbert Gaëlle, Bourlès Bernard.

We thank Reviewer 3 for his comments and suggestions that allowed improvements of our paper. We have made all needed modifications to make the figures easily understandable and conforming with general publications criteria (figures size, labels, etc). We have also made effort to make the main narrative of the manuscript easier to follow. A more in-depth analysis would have been obviously interesting but we first aimed to understand the different processes acting in the region. In addition, a more in-depth analysis of one or two particular processes would have prevented the description of the succession of the processes as a whole.

Response to specific comments:

RC: Why focus on this particular region? Is SST in it important for rainfall in a given region?

AC: The initial reason that motivates the study of the SST variability in the Cape-Lopez region is the observation in satellite SST data of cold coastal waters independent from those observed off shore in the cold tongue region around 10°W (see the map of satellite SST data for the 8 June 2005 shown on the Figure X1) which raises the question of the link of such cooling with the cold tongue development.

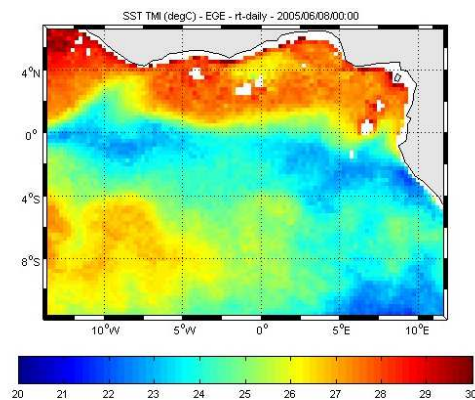


Figure X1: SST (°C) from TMI satellite data on 8 June 2005.

The equatorial region and the processes implied in the cold tongue development are largely studied contrary to the Cape-Lopez region. Other several studies focus on SST variability in more southern region such as Angola-Benguela front, but very few in the Cape-Lopez region. However, we thought that better describe the SST variability in the Cape-Lopez region is needed and interesting especially because of the numerous processes in play notably due to the presence of the coast and the proximity of the equator. In addition, some studies (such as DeCoëtlogon et al., 2010) suggest that at short time scale (a few days), more than half of the cold SST anomaly around the equatorial cooling could be explained by horizontal oceanic advection controlled by the winds. Therefore, a better understanding of the SST variability in CLR may also help to better understand the SST variability in equatorial region.

RC: How are conditions in the CLR related to the cold tongue farther west? What is the correlation between SST in the eastern box and in cold tongue box, for example?

AC: Given that the CLR and cold tongue region are submitted to the similar atmospheric forcing, the SST variability in both regions is quite close (cooling event at the same date). However, the processes responsible of the cooling differ from CLR region to cold tongue region due in particular to the presence of the coast. From many authors (Yu et al., 2006; Peter et al., 2006; Wade et al., 2011; Jouanno et al., 2011), the cooling in the cold tongue region would be regulated by a coupling between thermocline shoaling and subsurface dynamics such as turbulent mixing, vertical advection and entrainment, as well as horizontal advection.

In the CLR, we showed that upwelling processes are involved in particular around 3-4°S, as well as vertical current shear implying the SEC, which is enhanced during southerly wind bursts. Our analysis for the year 2005 and 2006 has also shown that during particular events (at the end of May and beginning of April 2006), a decrease of short wave radiation in CLR due to increased cloud cover contributes to the cooling. This phenomenon does not concern the equatorial region east of 0°W. In addition, for a given wind burst, the intensity of SST response in CLR and cold tongue region will modulate by subsurface conditions which are under the influence of equatorial Kelvin wave. For example in May 2005, the Kelvin wave reached the eastern coast while three wind bursts occurred, thus the thermocline was shallower in the east than west of 0°W. We also highlighted westward extension of cold

eastern upwelled water around 3°S through combined effects of westward surface currents, local wind influences and wave westward propagation which may contribute to the cooling in the southern edge of the cold tongue region.

Some lines about this have been added at the end of the section 4:

“In conclusion to the section 4, the SST variability in CLR at intraseasonal time scale is the result of combination between basin preconditioning by remotely forced shoaling of the thermocline via Kelvin wave, local mixing induced by current vertical shear, and upwelling processes in response to strong southerly winds. As highlighted for the 26-28 May 2005 and 2 April 2006 events, the net heat flux may also contribute to cool the surface waters, through enhanced cloud cover which decrease the incoming solar radiation. The cold upwelled waters around 3°S extend then westward from the eastern coast to near 20°W by combined effect of the westward propagating Rossby waves as well as vertical mixing and advection processes. The cool water may thus contribute to the cooling in the southern edge of the cold tongue region. Although the processes implied differ slightly due to the presence of the coast, the SST variability in CLR is quite close to the one in the equatorial cold tongue region (not shown), due to similar atmospheric forcing. However, for a given wind burst, the intensity of SST response in CLR and cold tongue region is modulated by subsurface conditions which are under the influence of equatorial Kelvin wave. In May 2005, the Kelvin wave reached the eastern coast while three wind bursts occurred. The thermocline was thus shallower in the east than west of 0°W, providing favorable subsurface conditions making the coupling between making the SST more reactive to wind intensification occurred during this month. In addition, the decrease short wave radiations due to enhanced cloud cover during the 26-28 May 2005 event or 2 April 2006, which contribute to the cooling in CLR, does not concern the equatorial region east of 0°W.”

RC: It is difficult to see the differences between Figs. 3 and 4. I suggest replacing with a figure showing differences, or adding a new figure.

AC: The figures 3 and 4 have been modified. The filtered SST (where the 30days-low pass filtered field has been removed to the total field) has been added in order to better highlight the cold episodes. In addition, a zoom over March-August period has been made for better clarity.

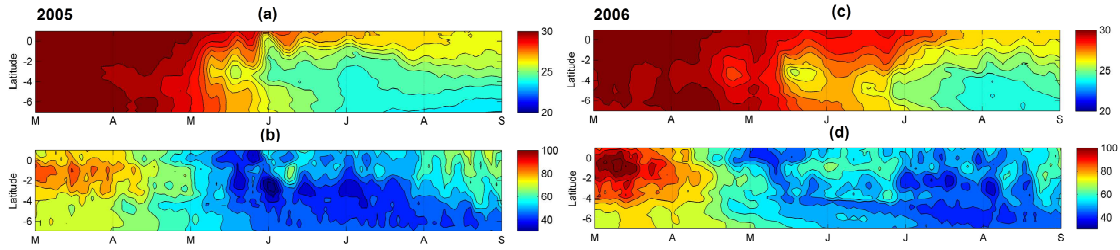


Figure 3: (a & c) Latitude-time diagram of the sea surface temperature ($^{\circ}\text{C}$) averaged between 5°E and 12°E ; (b & d) Latitude-time diagram of the 20°C -isotherm depth (m) averaged between 5°E and 12°E ; from 1st March to 31 August 2005 (left panels) and 2006 (right panels).

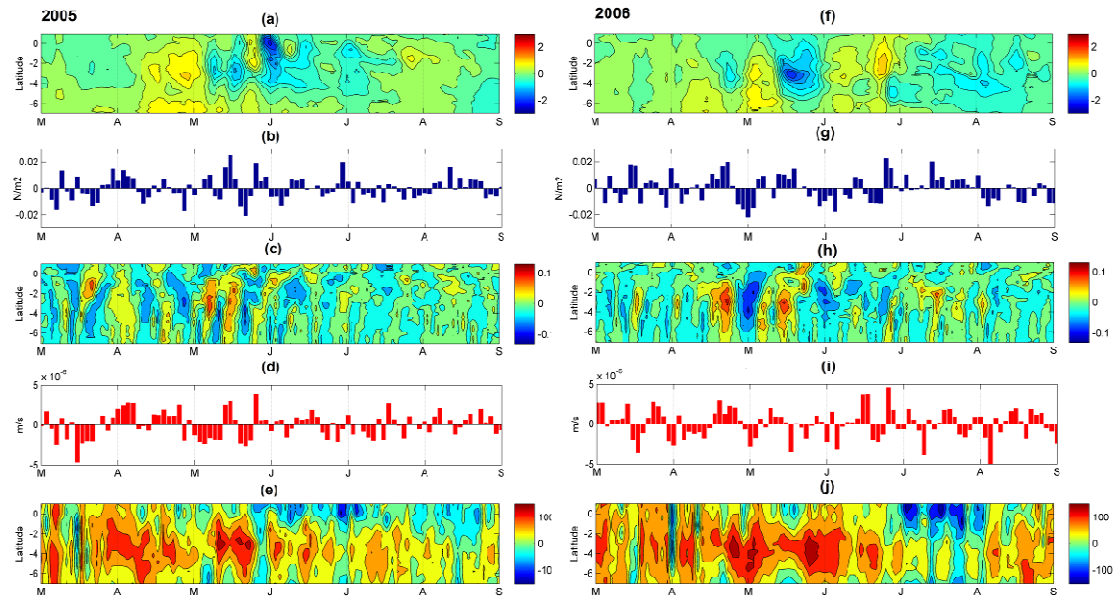


Figure 4: (a & f) Time-latitude diagram, from 7°S to 1°N , of the intraseasonal variations of sea surface temperature (in $^{\circ}\text{C}$) averaged between 5°E and 12°E ; (b & g) Time evolution of the intraseasonal variations of wind stress amplitude ($\text{N}\cdot\text{m}^{-2}$) averaged between 5°E and 12°E and between 3°S and 0°S ; (c & h) Latitude-time diagram of the intraseasonal variations of the maximum of the current vertical shear magnitude ($\text{m}\cdot\text{s}^{-1}$) averaged between 5°E and 12°E ; (d & i) Longitude-time diagram of the intraseasonal variations of Ekman Pumping ($\text{m}\cdot\text{s}^{-1}$) averaged between 7°S - 2°S and 5°E - 12°E . Ekman pumping values >0 indicate upwelling; (e & j) Latitude-time diagram of the net heat flux ($\text{W}\cdot\text{m}^{-2}$) averaged between 5°E and 12°E ; from 1st March to 31 August 2005 (left panels) and 2006 (right panels).

Modifications have also been made on the plot of 20°C -isotherm depths : weaker values of 20°C -isotherm depths indicate shallower thermocline to be consistent with the modifications made on the Fig.1, Fig.5, Fig.7, Fig. 9 and Fig. 13 in response to the other reviewers' comments.

RC: How are the results different (or confirm) previous studies of cold tongue variability? It's not clear.

AC: Our study does not focus on the cold tongue variability but, first, on SST variability more eastern, in the Cape-Lopez region. Marin et al. (2009) show that the cooling in 10°W-4°W region is the result of successive cooling events related to intraseasonal wind bursts. The two regions are under the influence of similar atmospheric forcing but the processes implied are rather different. We show that the SST in the CLR also reacts to the intraseasonal wind bursts. However, the processes responsible of the cooling differ from the CLR region to the cold tongue region due in particular to the presence of the coast (see our response to the previous question “How are conditions in the CLR related to the cold tongue farther west? What is the correlation between SST in the eastern box and in cold tongue box, for example?”).

The cold tongue region is mentioned in the second part of our paper when we focus on the mid-May 2005 wind burst and its impact on coastal monsoon onset. Indeed, we aim to describe the wind burst impacting the Cape-Lopez region at more global scale, so we analyzed its impact in the Cape-Lopez region and also in the cold tongue region through its role in West African Monsoon onset.

RC: Negative values in Figs. 3c, 4c to me mean shallower than normal thermocline, but it seems you are using the opposite sign so that positive values mean shallower. This is a little confusing. I recommend switching signs or making it clear in the Fig. 3 caption that negative means deeper. Also indicate in the caption that Ekman pumping values >0 indicate upwelling (I assume this is the case?).

AC: Thanks for this suggestion. We have modified the figures 3c and 4c in this sense and we have added that Ekman pumping values >0 indicate upwelling in the captions of the figures.

RC: Lines 279-292: Do zonal or meridional current variations dominate for the vertical shear, and are they driven by the anomalous meridional winds?

AC: The vertical shear is dominated by zonal current variations, related to the fluctuations of dominant southerly winds. We have modified the figure 3 and 4 where we plotted the vertical shear magnitude (see the response to the previous comment: “It is difficult to see the differences between Figs. 3 and 4. I suggest replacing with a figure showing differences, **or** adding a new figure.”). On the new figures, we also removed the 30-days low-pass filtered field to the total field.

RC: Lines 317-318: What do you mean by "steeper thermocline slope?" Do you mean stronger dT/dz within the thermocline, or shallower thermocline, or stronger horizontal gradients of thermocline depth...

AC: By 'steeper thermocline slope' we mean 'shallower thermocline'. We have clarified this in the text.

RC: Data/methods section: How are anomalies calculated? It is not stated anywhere, yet shown frequently in the figures. Was the mean seasonal cycle (monthly mean climatology) removed before making Fig. 5, Fig. 6?

AC: For the Figure 5, we applied a 30-days low-pass filter to the total field, averaged the result over 1998-2008 period and removed it to the total field of each year. Indications about how the calculations have been made for each figure have been added in the text.

RC: I don't see a good correspondence between Figs. 5 and 6. Maybe plotting anomalies from the seasonal cycle would help (if not done already). Otherwise, another method to validate the model's Z20 anomalies is needed.

AC: The figures 5 and 6 have been modified. Negative values of 20°C-isotherm depth now show shallower thermocline, to better highlight the correspondence between Fig. 5 and Fig. 6. The values plotted on Fig.5 are obtained by removing the 30-days low pass filtered field, averaged over 1998-2008 period to the total field.

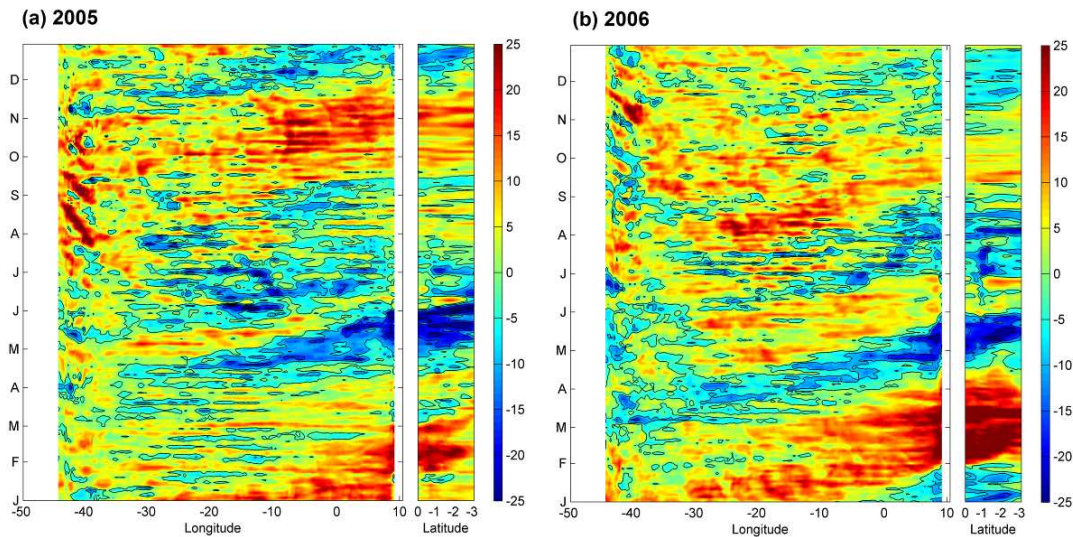


Figure 5: Time evolution of the intraseasonal variations anomalies of the 20° C-isotherm depth (m) along the equator (between 54° W and 12° E) and along 9° E (between the equator and 3° S) for 2005 (left) and 2006 (right). Negative values indicate a 20°C isotherm closer to the surface.

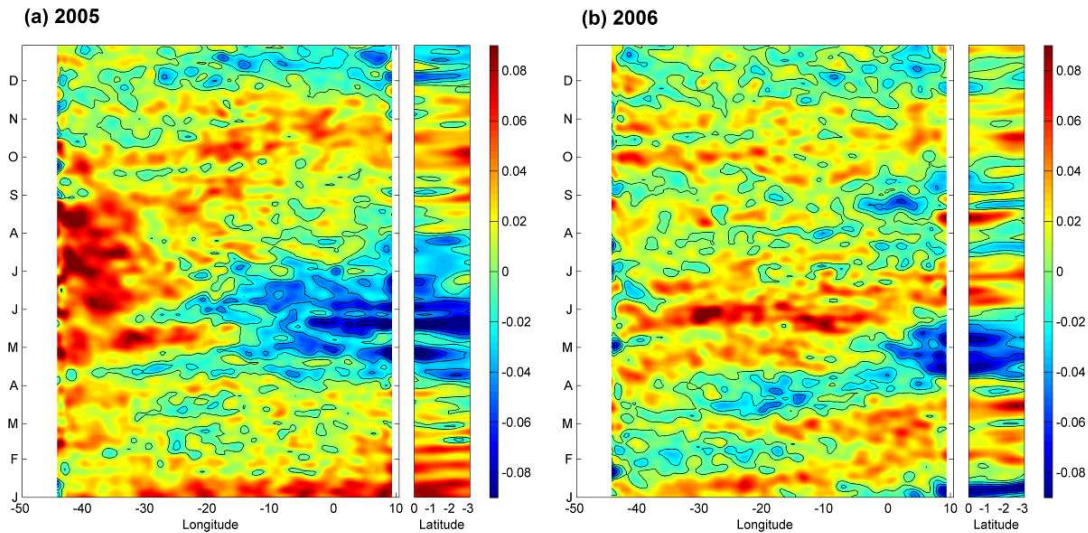


Figure 6: Time evolution of the sea level anomaly (m) along the equator (between 54° W and 12° E) and along 9° E (between the equator and 3° S) for 2005 (left), and 2006 (right) from AVISO data.

RC: Line 386: Do you mean Fig. 7c instead of Fig. 6c?

It's difficult to follow the discussion and reasoning on line 380-390. A figure showing spatial patterns of wind anomalies might help to visualize the changes in Ekman pumping and ITCZ shifts.

AC: Yes, sorry for that, we indeed mean Fig. 7c instead of Fig. 6c. We are not sure that it is necessary to add additional figure. We think that what we want to show is clearly visible on the plot of Fig. 7.

RC: What is the main result of the analysis discussed on p. 14-15? Why is it important that the southward movement of the ITCZ was more abrupt in 2005 and the winds following the event were different compared to 2006? Please state at the end of the section or mention that it will be discussed in later sections. If it didn't clearly affect later conditions, it should not be shown.

AC: In the previous section (4.2), we show that the intraseasonal cold SST variability in the CLR is the result of combination of local and remote forcing. The remote forcing is made through Kelvin wave eastward propagation associated with minimum z20 and SSH. For the years 2005, the May wind events was responsible to strong SST response, supported by favorable subsurface conditions. Since the subsurface conditions in the east is largely influenced by the arrival of Kelvin wave excited in the west, it seems to us interesting to better understand what are the atmospheric conditions associated with the Kelvin wave

excitation in the west and how they are different in 2005 and 2006. It is the aim of the section 4.2.2b. The main result of the analysis is that the anomalous strengthening of easterly winds occurs some days after the ITCZ to be at its southernmost location. In 2005, the ITCZ reaches its southernmost location through a sudden southward shift and returns to its initial position just after, whereas in 2006, the southernmost position of the ITCZ is reached less sharply and in the continuity of the evolution of the ITCZ's position, as it is moving southward. In order to better highlight the phenomenon discussed, we have plotted the intraseasonal variations anomalies (the 30 days low-pass filtered field averaged over 1998-2008 period have been removed to the total field) of wind stress magnitude, z20, and SLA on figure 7.

RC: Lines 414-415: How does Fig. 8 show an enhancement of SST cooling after May 10? It only shows SST averaged for May and for May 1-10.

AC: The enhancement of SST cooling after May 10 was deduced for the difference between the average over May and the average over May 1-10. For better clarity, we have modified the figure 8 and shown the mean for 1-12 May 2005 and for 14-30 May 2005. For comparison, the same calculation has been made for 2006.

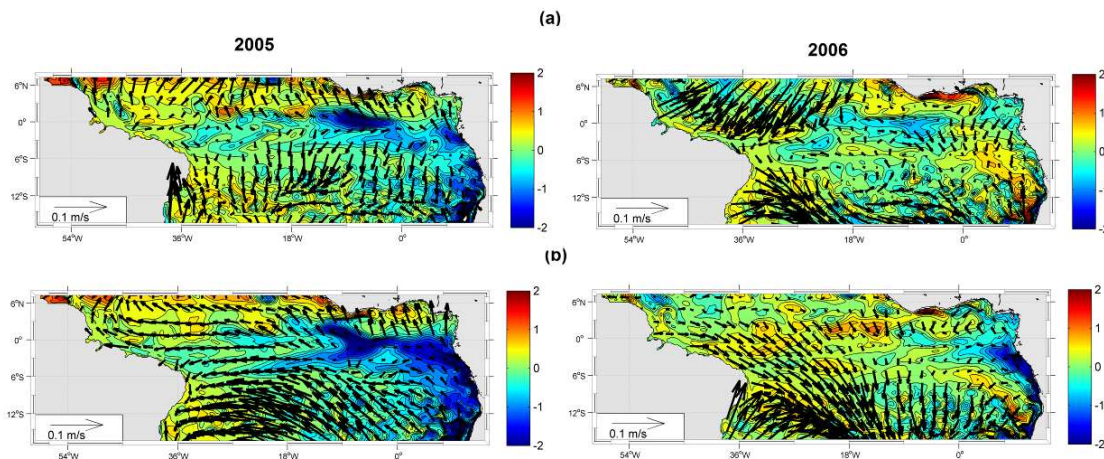


Figure 8: (a) Sea surface temperature anomalies ($^{\circ}$ C; color) superimposed with wind stress intensity anomalies (arrows) averaged over 1-12 May 2005 (before the mid-May event); (b) same but averaged between 14 May and 30 May 2005 (including the mid-May 2005 event).

RC: Figure 10: Why not show anomalies for all fields instead of only for winds?

It seems like sections 5.1.2 and 5.1.3 are not essential and could be eliminated.

AC: We modified the Figure 10 and decided to show the total field for all fields and to separate the wind pattern and the precipitation pattern for more visibility. The aim is to describe the atmospheric conditions associated to the mid-May event 2005.

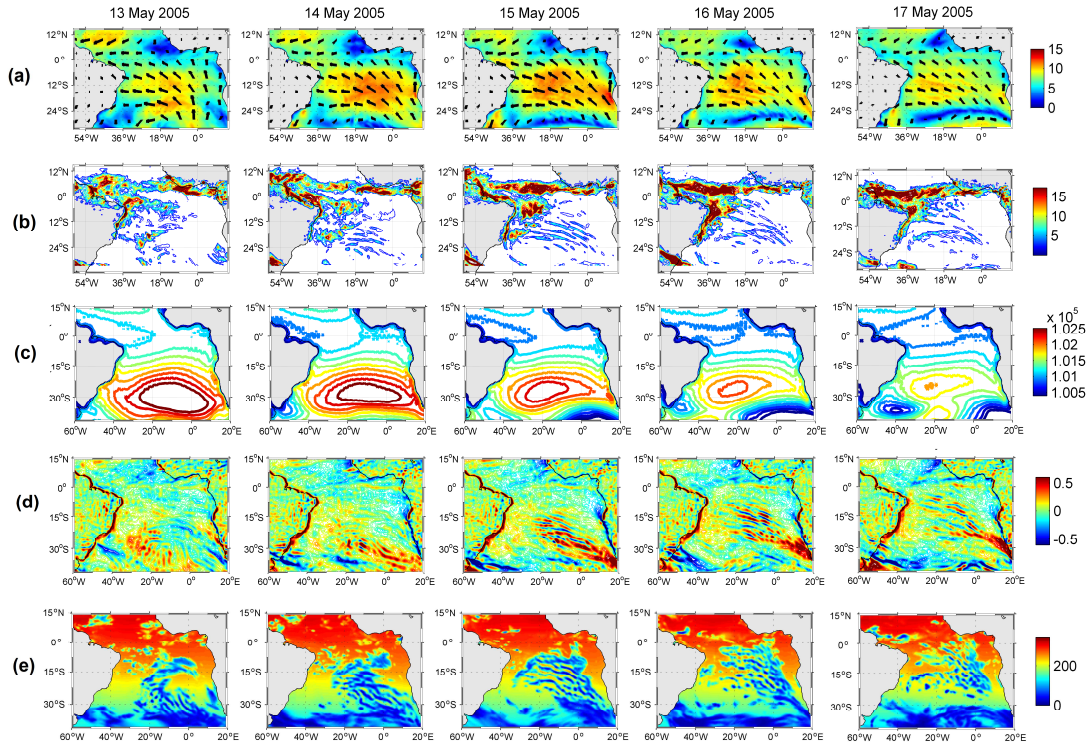


Figure 10: Daily-averaged, from 13 May to 17 May 2005 (left to right panels), of (a) wind magnitude (color field) (m.s^{-1}) superimposed with wind vectors from CFSR fields; (b) precipitation rate ($\text{kg.m}^{-2}/\text{day}^{-1}$) from CFSR fields; (c) surface pressure (hPa) from ERA-20C reanalysis; (d) wind speed curl (m.s^{-1}) computed from CFSR wind speed fields; and (e) downward short-wave radiation (W.m^{-2}) from CFSR fields.

However, we do not agree with the reviewer and do think that sections 5.1.2 and 5.1.3 are useful. Presently, the purpose of the second part of the paper is to better understand how the mid-May 2005 event is singular in addition to the anomalous strong southerly winds. These two sections show the particular conditions which accompanies the mid-May event. The section 5.1.2 shows that, through its time of occurrence and its impact on SST, the mid-May 2005 wind event has also an impact on precipitation pattern off northeast Brazil. In the section 5.1.3, we notice that the event is associated with atmospheric gravity wave which quickly propagates from south Atlantic to equatorial region, that highlights a way to carry momentum and energy of from South Atlantic region to tropical/equatorial region and raises

the question of the representation of the impact of such phenomenon on the SST variability in equatorial and eastern tropical region. So, we prefer to keep these sections.

Additional authors 'comments :

In addition to modifications listed above, modifications have been made to make the figures clearer and more easily understandable.

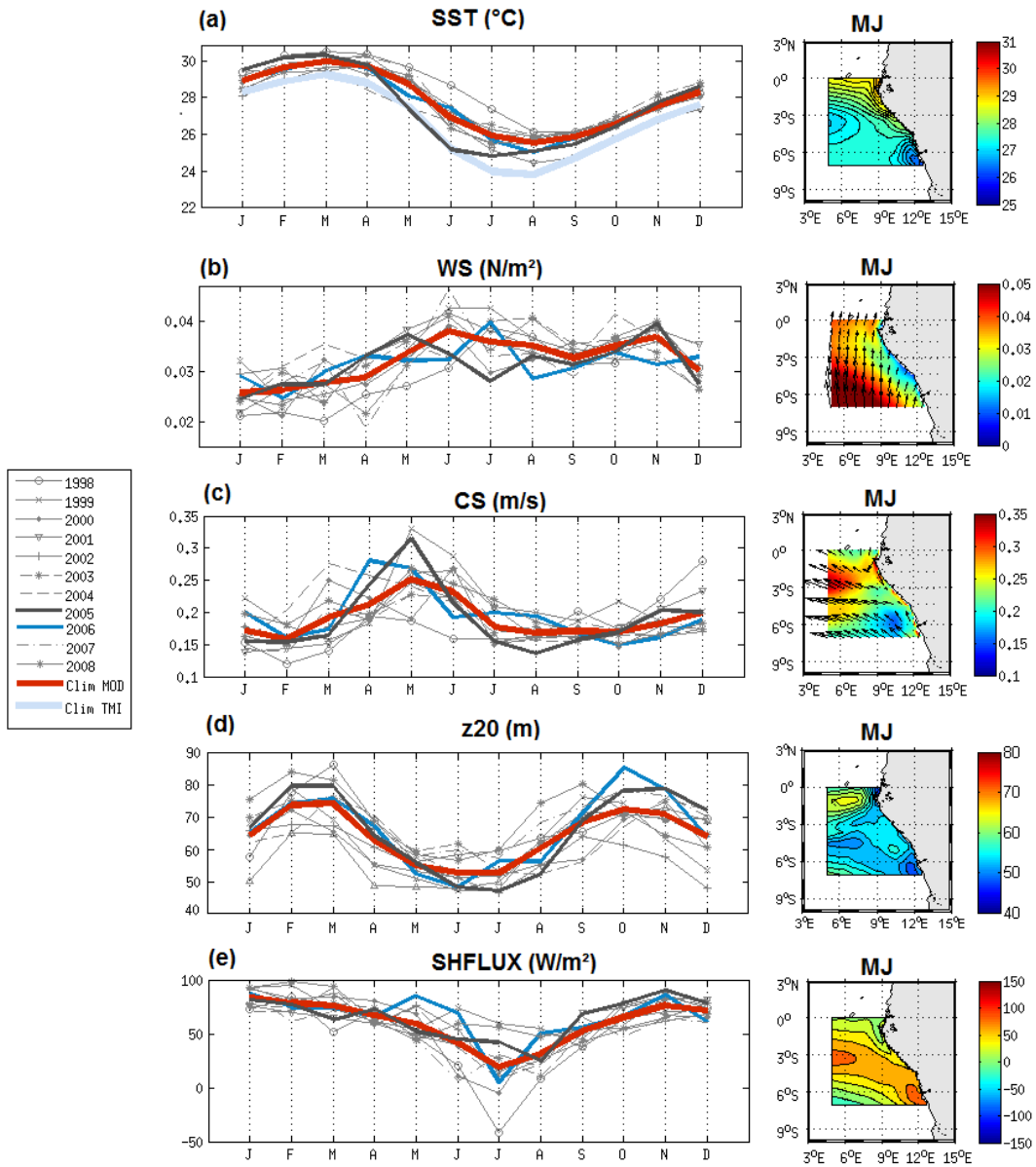


Figure 1: Monthly average of the (a) sea surface temperature (°C); (b) wind stress direction (vectors) and magnitude (color field) (N.m⁻²); (c) horizontal surface current direction (vectors) and speed (color field) (m.s⁻¹);

(d) 20° C-isotherm depth (m); and (e) surface heat flux ($\text{W}\cdot\text{m}^{-2}$; positive values indicate downward flux) from January to December from 1998 to 2008 and for the climatology (averaged over 1998-2008) simulated by the model (red curve) and from the observations : monthly average TMI 3-daily SST data (light blue curve in (a)); averaged over 5° E-14° E and 7° S-0° S. Right panel: maps of each variable over May-June.

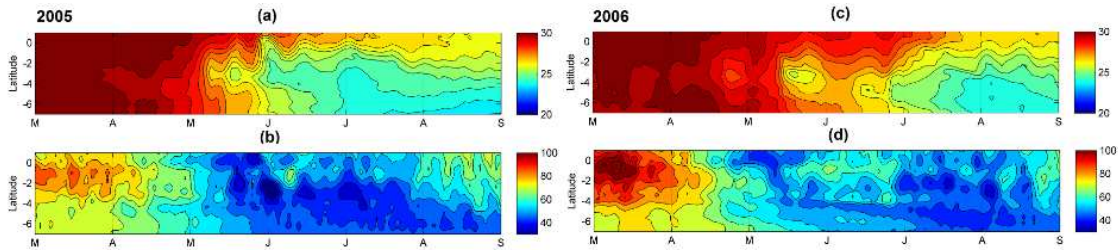


Figure 3: (a & c) Latitude-time diagram of the sea surface temperature ($^{\circ}\text{C}$) averaged between 5°E and 12°E; (b & d) Latitude-time diagram of the 20° C-isotherm depth (m) averaged between 5° E and 12° E; from 1st March to 31 August 2005 (left panels) and 2006 (right panels).

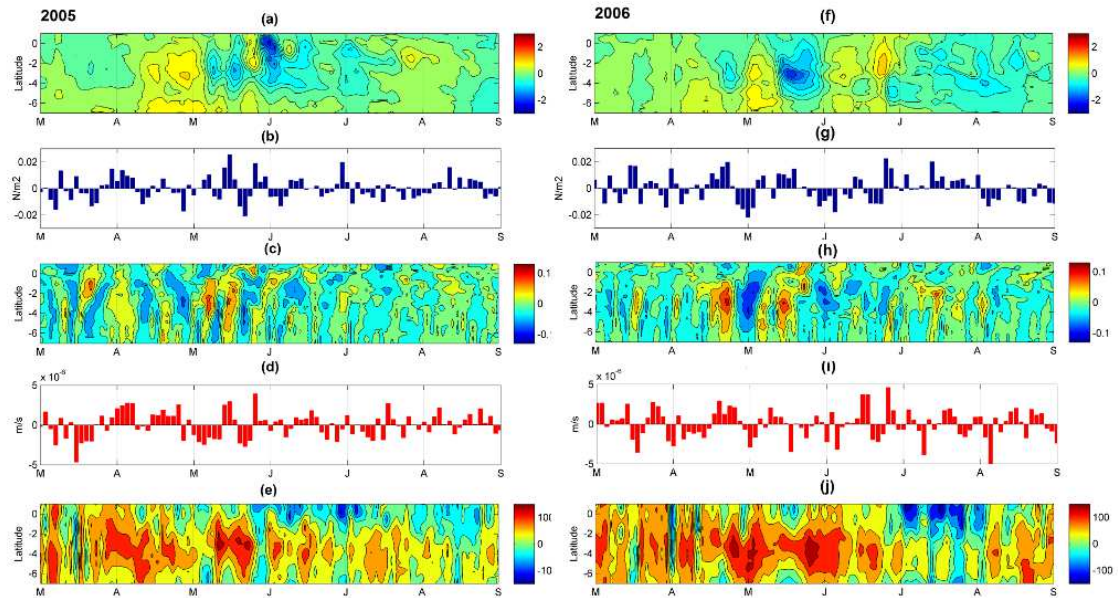


Figure 4: (a & f) Time-latitude diagram, from 7° S to 1° N, of the intraseasonal variations of sea surface temperature (in $^{\circ}\text{C}$) averaged between 5° E and 12° E; (b & g) Time evolution of the intraseasonal variations of wind stress amplitude ($\text{N}\cdot\text{m}^{-2}$) averaged between 5° E and 12° E and between 3° S and 0° S; (c & h) Latitude-time diagram of the intraseasonal variations of the maximum of the current vertical shear magnitude ($\text{m}\cdot\text{s}^{-1}$) averaged between 5° E and 12°E; (d & i) Longitude-time diagram of the intraseasonal variations of Ekman Pumping ($\text{m}\cdot\text{s}^{-1}$) averaged over the CLR. Ekman pumping values >0 indicate upwelling; (e & j) Latitude-time diagram of the net heat flux ($\text{W}\cdot\text{m}^{-2}$) averaged between 5° E and 12° E; from 1st March to 31 August 2005 (left panels) and 2006 (right panels).

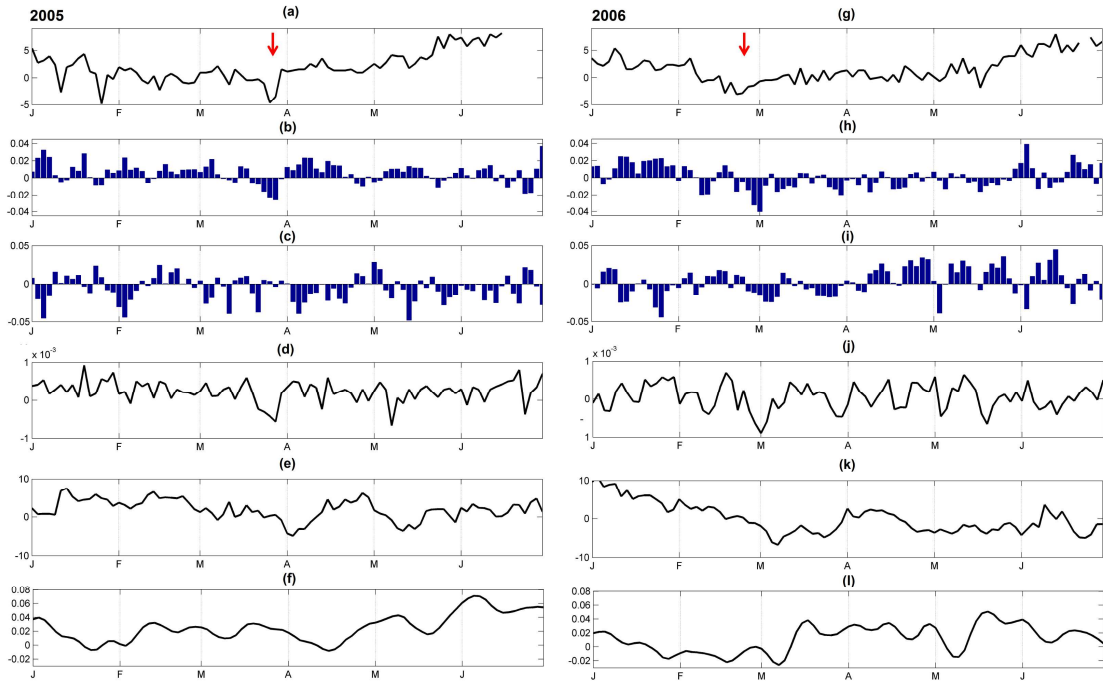


Figure 7: Time evolution, from 2-days averaged model outputs over Jan-June2005 (left) and Jan-June 2006 (right); of (a&g) the position (in latitude, between 5° S and 10° N) where the meridional wind stress value equal zero (indicator of the position of the ITCZ); (b&h) the meridional wind stress (N.m^{-2}) averaged between 50° W and 35° W and between 1° S and 1° N; (c&i) same as (b&h) but for zonal wind stress (N.m^{-2}); (d&j) the wind stress curl (N.m^{-2}); (e&k) the 20° C isotherm depth (m); (f&l) the sea level (m). The red arrow in (a&g) indicates the southward shift of the ITCZ before the excitation of the Kevin wave (see text). For each variable, the mean low-pass (> 1 month) filtered signal over 1998-2008 period has been removed to the total field.

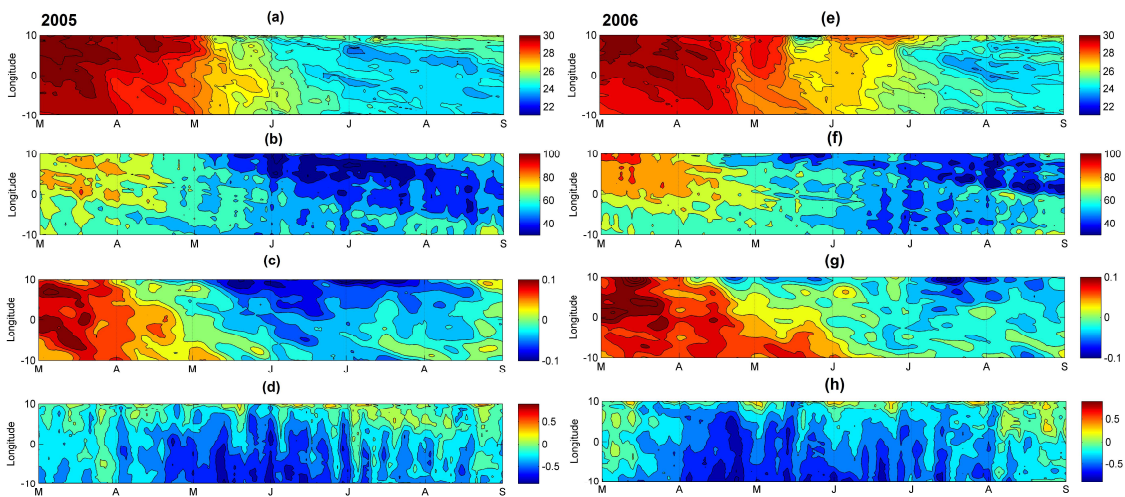


Figure 9: Time-longitude diagrams at 3° S between 10° W and 10° E, and from 2-days averaged model outputs from 1st March to 31 August 2005 and 2006, of (a & e) the sea surface temperature ($^{\circ}\text{C}$); (b & f) the 20° C isotherm-depth (m); (c & g) the sea level anomalies from AVISO data (m); and (d & h) the zonal component of surface velocity (m.s^{-1}).

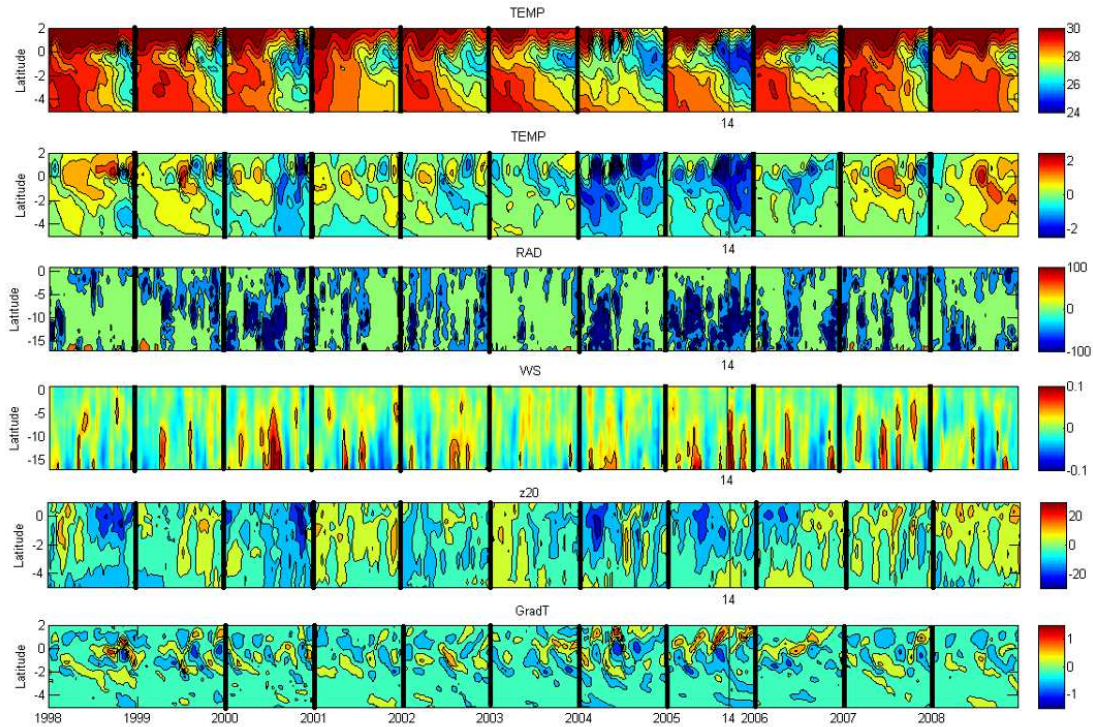


Figure 13: Time-latitude diagrams for April-May along the 1998-2008 period, of 2-days average, from top to bottom i) SST ($^{\circ}C$); ii) intraseasonal variations anomalies of SST ($^{\circ}C$); , iii) intraseasonal variations anomalies of wind stress magnitude ($N.m^{-2}$) from CFSR fields; iv) intraseasonal variations anomalies of short-wave radiation surface flux ($W.m^{-2}$) from CFSR fields; v) intraseasonal variations anomalies of 20 $^{\circ}C$ -isotherm depth (m) computed from the forced model SST; vi) intraseasonal variations anomalies of meridional SST gradient (every 0.5 $^{\circ}$ of latitude), from the forced model; averaged over 10 $^{\circ}$ W-6 $^{\circ}$ W. For all fields, except for the first SST field, the 30 days low-pass filtered annual field averaged over 1998-2008 period has been removed to the total field. The vertical black thin line indicates the date of 14 May, 2005.

Many English/grammar corrections have also been made in the text.